PERGAMON

Vision Research 39 (1999) 3513–3525

Vision Research

www.elsevier.com/locate/visres

Section 2

L, M and L–M hybrid cone photopigments in man: deriving λ_{max} from flicker photometric spectral sensitivities

Lindsay T. Sharpe [a,*], Andrew Stockman [b], Herbert Jägle [a], Holger Knau [a], Jeremy Nathans [c]

[a] *Forschungsstelle für Experimentelle Ophthalmologie, Röntgenweg 11, D-72076 Tübingen, Germany*
[b] *Department of Psychology, University of California San Diego, 9500 Gilman Drive, La Jolla, CA 92093-0109, USA*
[c] *Departments of Molecular Biology and Genetics, Neuroscience, and Ophthalmology, Howard Hughes Medical Institute, Johns Hopkins University School of Medicine, Baltimore, MA 21205, USA*

Received 4 November 1998; received in revised form 25 February 1999

Abstract

Using heterochromatic flicker photometry, we have measured the corneal spectral sensitivities of the *X*-chromosome-linked photopigments in 40 dichromats, 37 of whom have a single opsin gene in their tandem array. The photopigments encoded by their genes include: the alanine variant of the normal middle-wavelength sensitive photopigment, M(A180); the alanine and serine variants of the normal long-wavelength sensitive photopigment, L(A180) and L(S180); four different L–M hybrid or anomalous photopigments, L2M3(A180), L3M4(S180), L4M5(A180) and L4M5(S180); and two variants of the L-cone photopigment, encoded by genes with embedded M-cone exon two sequences, L(M2; A180) and L(M2; S180). The peak absorbances (λ_{max}) of the underlying photopigment spectra associated with each genotype were estimated by correcting the corneal spectral sensitivities back to the retinal level, after removing the effects of the macular and lens pigments and fitting a template of fixed shape to the dilute photopigment spectrum. Details of the genotype-phenotype correlations are summarized elsewhere (Sharpe, L. T., Stockman, A., Jägle, H., Knau, H., Klausen, G., Reitner, A. et al. (1998). *J. Neuroscience*, *18*, 10053–10069). Here, we present the individual corneal spectral sensitivities for the first time as well as details and a comparison of three analyses used to estimate the λ_{max} values, including one in which the lens and macular pigment densities of each observer were individually measured.

Keywords: M-cones; L-cones; Spectral sensitivity; Cone fundamental; Photopigments; Photopigment genes; Macular pigment; Lens pigment; Color matching; Single-gene dichromats; Dichromacy; Protanopes; Deuteranopes

1. Introduction

The three types of cone photopigment, each with different spectral sensitivity, are universally acknowledged to be the foundations of human trichromatic color vision. Among vision scientists, they are now most frequently referred to as short- (S-), middle- (M-) and long- (L-) wavelength-sensitive, according to the relative spectral positions of their peak sensitivities (i.e. their λ_{max} values). Two of these, the M- and L-cone photopigments, are encoded by genes that reside in a head-to-tail tandem array on the *X*-chromosome (reviewed in Nathans, Merbs, Sung, Weitz & Wang, 1992; Sharpe, Stockman, Jägle & Nathans, 1999). Each gene in the array consists of six coding regions, called exons, which are transcribed to produce the opsin or protein that binds with the chromophore, 11-*cis* retinal, to form the photopigment.

The near identity (96%) and juxtaposition of the coding regions of the M- and L-cone opsin genes (Nathans, Thomas & Hogness, 1986) give rise to frequent unequal homologous exchanges between them, resulting in the formation of hybrid or fusion genes. Some of the hybrid genes code for photopigments with absorbance spectrum lying between those of the normal M- and L-cone photopigments. Hybrid opsin genes are denoted as 5′M–3′L or 5′L–3′M to indicate which

* Corresponding author. Tel.: +49-7071-2983734; fax: +49-7071-295777.
E-mail address: ted.sharpe@uni-tuebingen.de (L.T. Sharpe)

0042-6989/99/$ - see front matter
PII: S0042-6989(99)00061-9

parental gene contributed sequences for their 5′ or upstream end and which contributed sequences for their 3′ or downstream end. Because unequal recombination is more likely to occur between exons rather than within them, both 5′M–3′L or 5′L–3′M hybrid opsin gene can conveniently be identified by the site at which the transition from an L-cone to an M-cone opsin gene occurs. Thus, L3M4, for example, indicates a 5′L–3′M hybrid gene in which exons 1–3 derive from an L-cone pigment gene and exons 4–6 from an M-cone pigment gene.

Experiments aimed at defining in vivo the spectral sensitivities (phenotypes) of the photopigments associated with such genotypes have often relied on psychophysical techniques, involving one or more of the following conditions: (i) the application of steady (Stiles, 1939; De Vries, 1948; Wald, 1964) or transient (e.g. King-Smith & Webb, 1974; Stockman, MacLeod & Vivien, 1993b) chromatic adaptation to favor the desired cone type while disadvantaging the unwanted cone types; (ii) the presentation of brief or flickering targets, such as in heterochromatic flicker photometry experiments, to avoid the intrusion of color-opponent processes in the detection process (for a review of procedures, see Stockman & Sharpe, 1999); and (iii) the use of red–green dichromatic observers, who lack one of the *X*-chromosome-linked photopigments (e.g. Pitt, 1935; Hecht, 1949; Willmer, 1950; Hsia & Graham, 1957; Mitchell & Rushton, 1971; Rushton, Powell & White, 1973; Smith & Pokorny, 1975; Alpern & Wake, 1977), to reduce the complications introduced by overlapping spectral sensitivities in normal observers.

In a study documented elsewhere (Sharpe, Stockman, Jägle, Knau, Klausen, Reitner et al., 1998a), we exploited all three of these conditions to make genotype–phenotype correlations. Using both chromatic adaptation and heterochromatic flicker photometry, we measured, for centrally viewed 2° in diameter fields, the photopigment spectral sensitivities of 40 male dichromats, 37 of whom have only a single opsin gene on their *X*-chromosome. We were able to identify nine normal and 5′L–3′M hybrid opsin photopigments, each of whose amino acid sequences were deduced from its gene sequences: L(A180), L(S180), L1M2(A180) or M(A180), L2M3(A180), L3M4(S180), L4M5(A180), L4M5(S180), L(M2; A180) and L(M2; S180). As part of the gene and photopigment description, it is parenthetically denoted whether the alanine (A180) or serine (S180) polymorphism at codon 180 is present, and whether a M-cone pigment gene exon 2 (M2) is embedded within an otherwise L-cone opsin gene (Sharpe et al., 1999).

Here, we present in full the individual spectral sensitivities measured in the 40 dichromats, thus allowing the reader to evaluate directly the reliability and inter-observer variability of the data. In addition, we present here, for the first time, the individually measured crystalline lens and macular pigment densities for each observer. Estimates of the lens and macular pigment densities are needed to correct the corneally measured spectral sensitivities back to the retinal level, so that the peak absorbances of the underlying photopigment spectra (i.e. the λ_{max} values) can be derived. The lens and macular pigments both alter spectral sensitivity by absorbing light mainly of short-wavelengths, and both vary substantially in density between individuals (see, for example, Wyszecki & Stiles, 1982; Stockman & Sharpe, 1999).

In the original study (Sharpe et al., 1998a), we used best-fitting lens and macular pigment densities to derive the λ_{max} values. Here we attempt to improve the λ_{max} estimates by replacing the best-fitting lens and macular pigment densities used in the fits with the individually measured (fixed) density values. Unfortunately, the measured densities proved to be too inaccurate.

2. Methods

2.1. Subjects

A total of 40 males with severe color vision deficiencies were recruited in Freiburg, Tübingen, and Vienna by word of mouth and by advertising in local newspapers and cinemas. All were native Germans or Austrians, except for approximately 15% who were natives of the Balkan peninsula. The males were between 16 and 45 years old with a mean age of 28 (see Table 1, column 3). To qualify for the study, each had to be phenotypically a dichromat in the red–green part of the visible spectrum. That is, he had to produce a Rayleigh match on a standard anomaloscope by merely adjusting the intensity of the yellow light, regardless of the red–green ratio (Rayleigh, 1881). Such matches are consistent with light absorption being mediated by a single type of photopigment in the middle- and long-wavelength region of the spectrum, where the Rayleigh equation applies. Red–green dichromats can be either protanopes, who lack the L-cone photopigment, or deuteranopes, who lack the M-cone photopigment. Protanopes produce characteristically different matches than deuteranopes owing to differences in the spectral sensitivity of their remaining M- or L-cone photopigment (for details of the individual matches, see Sharpe et al., 1998a, b).

2.2. Genotyping

Full details of the genotyping, including the deduced

amino acid sequences in exons 2–5 for all 40 dichromats, can be found in table 2 of Sharpe et al. (1998a).

2.3. Apparatus

Full details of the design and calibration of the Maxwellian-view optical system, used to measure the heterochromatic flicker photometric sensitivities as well as to estimate the lens and macular pigment densities, are provided in Sharpe et al. (1998a).

2.4. Procedure

2.4.1. Corneal spectral sensitivities

The heterochromatic flicker photometric procedures used to measure the corneal spectral sensitivities are fully described in Sharpe et al. (1998a). They will only be briefly summarised here. A 2° reference light (560 nm) was alternated at 25 Hz, or in preliminary measurements, at 16 Hz, in opposite phase with a superimposed test light, the wavelength of which was varied in

Table 1
Best-fitting photopigment λ_{max} values, lens and macular pigment densities according to the full spectrum analysis[a]

	Code	Age	$\lambda_{max} \pm$ S.E.	Lens density $\pm$ S.E. (400 nm)	Macular pigment density $\pm$ S.E. (460 nm)	RMS error	Genotype
1	HS2196	35	525.58 ± 0.68	1.81 ± 0.08	0.14 ± 0.04	0.07	L1M2(A180)
2	HS2234	42	528.80 ± 0.71	1.55 ± 0.06	0.26 ± 0.04	0.07	L1M2(A180)
3	HS2241	19	528.88 ± 0.74	1.71 ± 0.06	0.32 ± 0.04	0.09	L1M2(A180)
4	HS2303	45	529.69 ± 0.40	1.83 ± 0.05	0.61 ± 0.02	0.06	L1M2+M(A180)
5	HS2197	27	527.16 ± 0.52	1.82 ± 0.05	0.39 ± 0.07	0.07	L2M3(A180)
6	HS2201	39	528.84 ± 0.69	1.68 ± 0.06	0.01 ± 0.04	0.06	L2M3(A180)
7	HS2298	18	529.61 ± 0.67	1.81 ± 0.12	0.30 ± 0.03	0.09	L2M3(A180)
8	HS2288	24	529.73 ± 0.45	1.28 ± 0.03	0.28 ± 0.02	0.07	L2M3+M(A180)
9	HS2293	32	529.59 ± 0.53	1.54 ± 0.03	0.55 ± 0.03	0.07	L2M3+M(A180)
10	HS2188	30	530.68 ± 0.51	1.14 ± 0.04	0.73 ± 0.03	0.07	L3M4(S180)
11	HS2198	29	529.75 ± 0.49	1.39 ± 0.06	0.43 ± 0.03	0.08	L3M4(S180)
12	HS2235	23	530.71 ± 0.58	1.48*	0.08 ± 0.04	0.07	L3M4(S180)
13	HS2237	16	532.14 ± 0.51	1.57 ± 0.06	0.49 ± 0.03	0.08	L3M4(S180)
14	HS2307	23	534.15 ± 0.47	1.79 ± 0.04	0.44 ± 0.02	0.07	L3M4(S180)
15	HS2305	23	535.45 ± 0.51	1.60 ± 0.04	0.25 ± 0.02	0.08	L4M5(A180)
16	HS2202	29	534.18 ± 0.40	1.25 ± 0.05	0.34 ± 0.02	0.07	L4M5(S180)
17	HS2219	24	556.88 ± 0.49	1.31 ± 0.04	0.35 ± 0.02	0.08	L(M2;A180)
18	HS2182	27	557.79 ± 0.51	1.15 ± 0.04	0.44 ± 0.03	0.07	L(A180)
19	HS2232	25	556.81 ± 0.77	1.48[b]	0.27 ± 0.04	0.07	L(A180)
20	HS2245	23	558.13 ± 1.44	1.62 ± 1.02	0.36 ± 0.09	0.09	L(A180)
21	HS2247	43	558.78 ± 1.46	1.14 ± 1.03	0.48 ± 0.09	0.09	L(A180)
22	HS2313	22	558.52 ± 0.23	1.66 ± 0.02	0.28 ± 0.01	0.04	L(M2;S180)
23	HS2171	27	559.27 ± 0.34	1.82 ± 0.04	0.56 ± 0.02	0.06	L(S180)
24	HS2173	28	560.61 ± 0.68	1.46 ± 0.05	0.83 ± 0.03	0.08	L(S180)
25	HS2176	22	559.95 ± 0.57	1.51 ± 0.05	0.44 ± 0.03	0.08	L(S180)
26	HS2177	20	559.92 ± 0.59	1.62 ± 0.06	0.26 ± 0.03	0.07	L(S180)
27	HS2181	23	561.76 ± 0.41	1.44 ± 0.04	0.48 ± 0.02	0.07	L(S180)
28	HS2184	27	558.84 ± 0.59	0.81 ± 0.05	0.28 ± 0.02	0.08	L(S180)
29	HS2185	27	560.58 ± 0.50	0.97 ± 0.04	0.37 ± 0.02	0.07	L(S180)
30	HS2218	25	560.53 ± 0.52	1.13 ± 0.03	0.21 ± 0.02	0.07	L(S180)
31	HS2220	42	560.54 ± 0.60	1.45 ± 0.07	0.37 ± 0.03	0.07	L(S180)
32	HS2221	27	558.94 ± 0.65	0.86 ± 0.08	0.17 ± 0.03	0.07	L(S180)
33	HS2229	25	558.01 ± 0.56	1.47 ± 0.05	0.38 ± 0.02	0.07	L(S180)
34	HS2231	30	559.23 ± 0.72	1.29 ± 0.07	0.43 ± 0.03	0.06	L(S180)
35	HS2243	23	559.11 ± 0.97	1.48[b]	0.01 ± 0.05	0.08	L(S180)
36	HS2249	22	561.76 ± 0.72	1.48[b]	0.42 ± 0.05	0.06	L(S180)
37	HS2299	32	561.87 ± 0.32	1.67 ± 0.03	0.50 ± 0.01	0.05	L(S180)
38	HS2304	26	562.09 ± 0.31	1.76 ± 0.02	0.38 ± 0.01	0.05	L(S180)
39	HS2322	41	561.42 ± 0.43	1.70 ± 0.03	0.58 ± 0.02	0.06	L(S180)
40	HS2357	37	560.32 ± 0.44	1.66 ± 0.04	0.42 ± 0.02	0.07	L(S180)

[a] Columns 4–7, best-fitting photopigment λ_{max} values (in nm), lens densities at 400 nm, peak macular pigment densities at 460 nm and root-mean-squared (RMS) errors for the fit of the full spectrum model (Eqs. (1), (2) and (3a)) to each subject's spectral sensitivity data. The $\pm$ S.E. values are plus and minus the standard error of each fitted parameter. The subject code (column 2), age (column 3) and genotype (column 8) are also listed.

[b] In four subjects (HS2232, HS2243, HS2249 and HS2235), in whom short-wavelength measurements below 470 nm were not completed, the lens density could not be reliably estimated. For them, we fixed the density at 1.48, the mean density value for all subjects.

5-nm steps over the spectrum from 400 to 700 nm. The two targets were presented on a 430-nm field of 11.00 log quanta s^{-1} deg^{-2} (3.08 log photopic td or 4.71 log scotopic td), which saturated the rods and, together with the high flicker rate, obviated the contribution of the S-cones.

2.4.2. Lens pigment

Lens pigment densities were estimated from 1-Hz rod thresholds measured at test wavelengths of 400, 420, 460 and 500 nm at an eccentricity of 13° in the temporal retina by comparing them with the corresponding values of the standard $V'(\lambda)$ scotopic luminosity function (table I(4.3.2) of Wyszecki and Stiles (1982)). We assumed that differences between the shape of $V'(\lambda)$ and the rod functions for each individual subject reflect differences in lens absorption in the violet (essentially the method of Ruddock (1965)). Each set of rod spectral sensitivity measurements was preceded by 40 min of dark adaptation. A dim 620 nm background of 6.25 log quanta s^{-1} deg^{-2} (-1.63 log sc td or -0.31 log ph td) was used, mainly to aid fixation. The scotopic spectral sensitivities were averaged from 20 settings: four separate runs of five threshold settings per target wavelength.

To estimate the lens density, we assumed the lens optical density spectrum of van Norren and Vos (1974), slightly modified by Stockman, MacLeod and Johnson (1993a). We also allowed a vertical shift of the log spectral sensitivity curves in order to account for wavelength-independent changes in overall sensitivity between subjects. With the use of a standard curve-fitting algorithm, we found: (1) the value by which the lens density spectrum should be multiplied before being added to or subtracted from each subject's data; and (2) the vertical shift that together with (1) minimized the squared deviations between the subject's data and $V'(\lambda)$. This estimate of lens density yields the relative difference in density between each of our subjects and the mean density of the 50 observers upon which the $V'(\lambda)$ function was based. To provide an absolute estimate of lens density, which we needed for the analysis of spectral sensitivity, we assumed that the mean density of the 50 observers upon which the $V'(\lambda)$ function is based was the same as the mean density for our 40 observers obtained from the best-fitting lens density analysis (i.e. 1.48 at 400 nm). Arbitrarily, we report lens densities relative to the density at 400 nm (see Tables 1 and 2).

2.4.3. Macular pigment

We estimated macular pigment density by comparing the 25-Hz flicker photometric sensitivities made at 13° in the periphery at 440, 460, 480, 500, 520, 540 and 560 nm with the corresponding sensitivities made centrally. Again, the targets were presented on a 430-nm field of 11.00 log quanta sec^{-1} deg^{-2} (3.08 log photopic td or 4.71 log scotopic td). We ignored the changes in photopigment optical density with eccentricity, and accounted for the differences in shape between the central and peripheral spectral sensitivity curves solely in terms of a change in macular pigment (e.g. Stiles, 1953; see also Sharpe, Stockman, Knau & Jägle, 1998b). We assumed the macular pigment density spectrum of Vos (1972), and allowed a vertical shift in log sensitivity between the central and less sensitive peripheral data. With the use of a standard curve-fitting algorithm, we found: (1) the factor by which the macular pigment density spectrum should be multiplied before being added to each subject's central data; and (2) the vertical shift that together with (1) minimized the squared deviations between the subject's central and peripheral data.

2.5. Analysis of spectral sensitivity data

The λ_{max} of each subject's L-, M- or L–M hybrid spectral sensitivity was estimated by fitting a photopigment template of fixed shape, defined by a fifth-order polynomial, to their flicker photometer data corrected to photopigment optical density spectra. As described in Sharpe et al. (1998a), the log photopigment optical density, $\log[P_{OD}(x)]$, spectrum normalized to zero peak, is:

$$\log[P_{OD}(x)] = a + \frac{b}{x} + \frac{c}{x^2} + \frac{d}{x^3} + \frac{e}{x^4} + \frac{f}{x^5}, \quad (1)$$

where x is $\log(\lambda)$, $a = 3593840.5764$, $b = -48574668.0585$, $c = 262378945.6275$, $d = -708007074.0766$, $e = 954435497.8303$, $f = -514228901.1364$, and λ is the wavelength in nm.

Three different fits with the photopigment template (Eq. (1)) were obtained: (i) a full-spectrum fit with best-fitting macular and lens densities; (ii) a full-spectrum fit with individually measured (fixed) macular and lens densities; and (iii) a partial-spectrum fit (≥ 520 nm).

2.5.1. Full-spectrum fit (with best-fitting lens and macular pigment densities)

The initial fit of the photopigment template (Eq. (1)) to the data was carried out in the single fitting procedure defined by Eqs. (2) and (3a):

$$S_{receptor}(x) = 1 - 10^{-0.5P_{OD}(x+\Delta x)}, \text{ and} \quad (2)$$

$$\log[S_{cornea}(x)] = \log[S_{receptor}(x)] + a\,lens_{OD}(x) + b\,mac_{OD}(x) + c_n. \quad (3a)$$

In Eq. (2), the template, $P_{OD}(x)$, is shifted by Δx log nm along the log wavelength scale and adjusted to a peak photopigment optical density of 0.5 (see Stock-

Table 2
Best-fitting photopigment λ_{max} values according to an analysis employing individually measured lens and macular pigment densities and according to a partial spectrum ($\geq$520 nm) analysis[a]

	Code	Measured lens density (400 nm)	Measured macular pigment density (460 nm)	$\lambda_{max} \pm$ S.E. measured lens and macular pigment densities	RMS error	$\lambda_{max} \pm$ S.E. partial spectrum	RMS error	Genotype
1	HS2196	2.18 ± 0.08	0.32 ± 0.11	522.15 ± 0.64	0.10	525.50 ± 0.77	0.07	L1M2(A180)
2	HS2234	1.71 ± 0.10	0.27 ± 0.16	527.87 ± 0.58	0.08	528.21 ± 0.60	0.07	L1M2(A180)
3	HS2241	XL[b] *1.70*	0.35 ± 0.07	528.52 ± 0.56	0.09	528.35 ± 0.83	0.09	L1M2(A180)
4	HS2303	1.78 ± 0.17	0.60 ± 0.12	529.42 ± 0.27	0.06	529.99 ± 0.36	0.06	L1M2+M(A180)
5	HS2197	1.80 ± 0.05	0.17 ± 0.10	530.10 ± 0.46	0.09	527.69 ± 0.49	0.07	L2M3(A180)
6	HS2201	1.81 ± 0.07	−0.09 ± 0.10	528.69 ± 0.51	0.06	528.56 ± 0.48	0.06	L2M3(A180)
7	HS2298	1.47 ± 0.08	0.38 ± 0.07	529.31 ± 0.43	0.09	530.10 ± 0.57	0.09	L2M3(A180)
8	HS2288	1.53 ± 0.03	0.37 ± 0.05	527.81 ± 0.33	0.08	529.50 ± 0.46	0.07	L2M3+M(A180)
9	HS2293	1.85 ± 0.13	0.68 ± 0.11	526.20 ± 0.50	0.10	529.85 ± 0.47	0.07	L2M3+M(A180)
10	HS2188	1.27 ± 0.10	0.76 ± 0.01	530.32 ± 0.39	0.07	530.47 ± 0.48	0.07	L3M4(S180)
11	HS2198	1.40 ± 0.08	0.56 ± 0.13	528.37 ± 0.40	0.08	529.51 ± 0.66	0.08	L3M4(S180)
12	HS2235	XLM	XLM			530.43 ± 0.60	0.07	L3M4(S180)
13	HS2237	1.20 ± 0.12	XM[b] *0.49*	533.09 ± 0.56	0.09	532.47 ± 0.58	0.08	L3M4(S180)
14	HS2307	1.68 ± 0.05	0.49 ± 0.06	536.12 ± 0.36	0.08	534.26 ± 0.47	0.07	L3M4(S180)
15	HS2305	1.68 ± 0.07	0.34 ± 0.04	533.69 ± 0.37	0.09	535.36 ± 0.45	0.08	L4M5(A180)
16	HS2202	1.18 ± 0.08	0.24 ± 0.10	535.52 ± 0.32	0.07	533.91 ± 0.27	0.07	L4M5(S180)
17	HS2219	1.38 ± 0.13	0.47 ± 0.10	555.39 ± 0.43	0.08	556.17 ± 0.50	0.08	L(M2;A180)
18	HS2182	1.32 ± 0.02	0.54 ± 0.07	556.16 ± 0.46	0.08	557.70 ± 0.64	0.07	L(A180)
19	HS2232	1.67 ± 0.10	0.11 ± 0.08	558.21 ± 0.73	0.08	556.99 ± 0.82	0.07	L(A180)
20	HS2245	XL	0.28 ± 0.11			558.28 ± 0.85	0.09	L(A180)
21	HS2247	XL	−0.07 ± 0.11			558.50 ± 0.60	0.09	L(A180)
22	HS2313	1.33 ± 0.03	0.06 ± 0.06	562.47 ± 0.42	0.09	558.78 ± 0.26	0.04	L(M2;S180)
23	HS2171	2.28 ± 0.05	0.80 ± 0.05	555.90 ± 0.47	0.10	559.88 ± 0.29	0.06	L(S180)
24	HS2173	1.65 ± 0.10	1.01 ± 0.17	558.08 ± 0.64	0.09	560.54 ± 0.79	0.08	L(S180)
25	HS2176	1.45 ± 0.10	0.55 ± 0.05	559.50 ± 0.48	0.08	559.95 ± 0.45	0.08	L(S180)
26	HS2177	1.71 ± 0.05	0.39 ± 0.16	558.34 ± 0.54	0.08	560.30 ± 0.66	0.07	L(S180)
27	HS2181	1.63 ± 0.02	0.51 ± 0.07	560.79 ± 0.37	0.10	561.90 ± 0.51	0.07	L(S180)
28	HS2184	1.71 ± 0.10	0.22 ± 0.08	556.67 ± 0.90	0.15	558.06 ± 0.67	0.08	L(S180)
29	HS2185	1.03 ± 0.07	0.50 ± 0.07	558.60 ± 0.45	0.08	560.05 ± 0.43	0.07	L(S180)
30	HS2218	1.20 ± 0.07	0.24 ± 0.16	560.01 ± 0.42	0.07	559.92 ± 0.46	0.07	L(S180)
31	HS2220	XLM	XLM			560.59 ± 0.67	0.07	L(S180)
32	HS2221	XL[b] *0.87*	0.19 ± 0.07	558.85 ± 0.55	0.07	558.30 ± 1.05	0.07	L(S180)
33	HS2229	1.47 ± 0.15	0.45 ± 0.07	556.93 ± 0.45	0.07	557.72 ± 0.54	0.07	L(S180)
34	HS2231	1.80 ± 0.10	0.09 ± 0.07	562.08 ± 1.24	0.11	559.01 ± 0.68	0.06	L(S180)
35	HS2243	XL	0.30 ± 0.15			559.11 ± 1.02	0.08	L(S180)
36	HS2249	XL	0.51 ± 0.13			561.65 ± 0.59	0.06	L(S180)
37	HS2299	1.58 ± 0.02	0.50 ± 0.07	562.21 ± 0.27	0.05	562.35 ± 0.38	0.05	L(S180)
38	HS2304	1.45 ± 0.07	0.21 ± 0.05	565.59 ± 0.55	0.09	562.70 ± 0.38	0.05	L(S180)
39	HS2322	1.38 ± 0.05	0.59 ± 0.18	562.47 ± 0.47	0.08	562.22 ± 0.48	0.06	L(S180)
40	HS2357	1.42 ± 0.08	0.19 ± 0.08	564.54 ± 0.62	0.11	561.12 ± 0.45	0.07	L(S180)

[a] Columns 3–6, measured lens density, measured macular pigment density and best-fitting photopigment λ_{max} values (in nm) and root-mean-squared (RMS) errors for the fit of the full-spectrum model [Eqs. (1), (2) and (3a)] to each subject's mean spectral sensitivity data incorporating their individually measured lens and macular pigment density values. Columns 7 and 8, best-fitting photopigment λ_{max} values and root-mean-squared (RMS) errors for the fit of the partial-spectrum ($\geq$520 nm) model [Eqs. (1), (2) and (3b)] to each subject's mean spectral sensitivity data. For the λ_{max} estimates, the ± S.E. values are plus and minus the standard error of the fitted photopigment template. For the measured densities, they are for the fit of the lens or macular pigment optical density spectra to the data (see Section 2). The subject code (column 2) and subject genotype (column 9) are also listed. XLM, no lens or macular pigment density measurements made.

[b] XL or XM, no lens or macular pigment density measurements made, respectively, the missing density has been replaced with the best-fitting one (italics), which was found by fixing the known macular (XL) or lens (XM) density at its measured value and allowing the unknown density to vary to find its best-fitting value. XL, no lens measurements made, the lack of short-wavelength data for this subject made the derivation of the best-fitting lens density impracticable.

man & Sharpe, 1999) to give the spectral sensitivity at the retinal level, $S_{\text{receptor}}(x)$. In preliminary trials, we also attempted to optimize the peak photopigment optical density (rather than assuming the fixed value of 0.5 in Eq. (2), but found that it was too poorly constrained. We therefore fixed it at 0.5 for each observer (see Stockman & Sharpe, 1999). In Eq. (3a), the spectral sensitivity at the retina, $S_{\text{receptor}}(x)$, is corrected to the cornea, $S_{\text{cornea}}(x)$, by restoring the filtering effects of the lens pigment, $a\text{lens}_{\text{OD}}(x)$, and macular pigment, $b\text{mac}_{\text{OD}}(x)$. We assumed the lens pigment density spectrum [$\text{lens}_{\text{OD}}(x)$] of van Norren and Vos (1974), slightly modified by Stockman et al. (1993a), and a macular pigment density spectrum [$\text{mac}_{\text{OD}}(x)$] based on the Vos (1972) estimate. Vertical shifts (c_{n}) were estimated for each of the n runs carried out by each subject. The lens density multiplier (a), the macular pigment density multiplier (b), the template shift (Δx) and vertical shifts (c_{n}) are all best-fitting values determined by the fit of the model defined by Eqs. (1), (2) and (3a) to each set of data. Each fit was carried out using the Marquardt–Levenberg algorithm implemented in SigmaPlot (Jandel Scientific).

2.5.2. Full-spectrum fit (with measured lens and macular pigment densities)

We also carried out the full-spectrum fit with individually measured estimates of the individual macular and lens pigment densities. That is, we used Eq. (3a) as in the full-spectrum fit (Section 2.5.1), but with a and b fixed at the measured values (see Table 2).

2.5.3. Partial-spectrum fit ($\geq$ 520 nm)

In this analysis, the fit was carried out only for measurements made at wavelengths ≥ 520 nm. In this region, the macular pigment plays little role, and the lens is relatively transparent (having an average optical density of only 0.10 log unit at 520 nm that declines with wavelength). Thus Eq. (3a) can be replaced by Eq. (3b):

$$\log[S_{\text{cornea}}(x)] = \log[S_{\text{receptor}}(x)] + \text{lens}_{\text{OD}}(x) + \text{mac}_{\text{OD}}(x) + c \qquad (3b)$$

The lens and macular pigment densities were fixed at the mean population densities obtained in the full-spectrum fit (Section 2.5.1). Thus, $\text{lens}_{\text{OD}}(x)$ is 1.48 at 400 nm and $\text{mac}_{\text{OD}}(x)$ is 0.37 at peak (see Table 1). The average data for each subject were used for this fit, so that there is only a single vertical shift (c). The template shift (Δx) and vertical shift (c) are best-fitting values determined by the fit of the model defined by Eqs. (1), (2) and (3b)) to the mean data (≥ 520 nm) for each subject.

3. Results

3.1. Genotype

The 40 dichromats studied here were originally classified as protanopes or deuteranopes according to the characteristic slope of the regression line fitted through their Rayleigh matches (for details, see Sharpe et al., 1998a). They were then categorized (see the rightmost column in Tables 1 and 2) according to the amino acid sequences of their X-linked cone photopigment (or photopigments) as deduced from its (their) gene sequences. Of the 24 single gene deuteranopes, four had L(A180) genes, one an L(M2;A180) gene, 18 L(S180) genes and one an L(M2;S180) gene. Of the 13 single-gene protanopes, three had L1M2(A180) genes, three L2M3(A180) genes, five L3M4(A180) genes, one an L4M5(A180) gene and one an L4M5(S180) gene. In addition, three protanopes had multiple genes, one with an L1M2(A180) and an M(A180) gene, and two with an L2M3(A180) and an M(A180) gene.

3.2. Spectral sensitivities

Foveal spectral sensitivities were determined in all 40 subjects by heterochromatic flicker photometry. However, in four of the observers (HS2232, HS2243, HS2249 and HS2235) short-wavelength measurements below 470 nm could not be completed (see Table 1). Figs. 1–5 show the individual spectral sensitivity data grouped according to genotype. The continuous lines fitted to each data set are the predictions of the full-spectrum model with best-fitting lens and macular densities. In general, this model provides a good description of the spectral data, despite large individual differences in the data due to inter-observer variability in the lens and macular pigment densities (see, for example, Fig. 4, in which all observers have the same photopigment, but very different spectral sensitivities at short wavelengths).

The number of data points measured for each subject depended on their availability. Six subjects did not complete the short-wavelength measurements. Given that the subjects were naïve, the overall quality of the data is good. Data treatment is discussed in detail elsewhere (see Sharpe et al., 1998a).

3.3. Macular pigment densities

We estimated the macular pigment densities from the differences between cone spectral sensitivities measured centrally and peripherally (see Section 2). The density estimates are given in Table 2, as the density of the pigment at 460 nm, which is close to the wavelength of peak density.

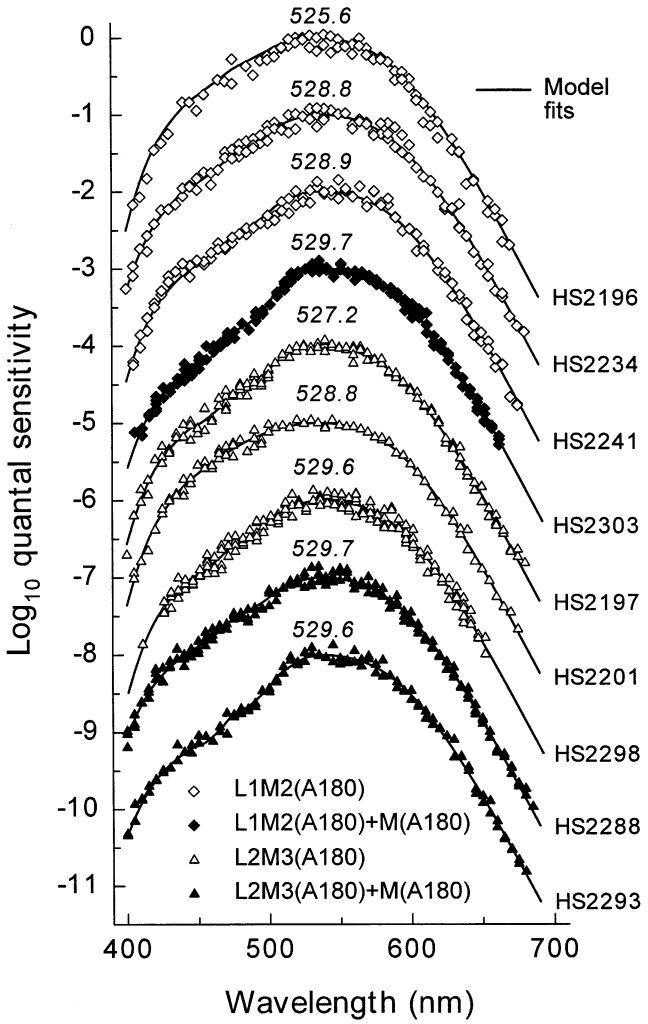

Fig. 1. Cone spectral sensitivity data for nine protanopes: three with a single L1M2(A180) (◇); one with an L1M2(A180) plus an M(A180) gene (◆); three with a single L2M3(A180) gene (△); and two with an L2M3(A180) plus an M(A180) gene (▲). The fits of the full-spectrum model (see text) are shown by the continuous lines; the λ_{max} of the fitted photopigment template is given above each curve.

Estimates of the macular pigment densities were obtained in all but three of the dichromats (HS2235, HS2237, HS2220). The macular pigment densities at 460 nm are listed in Table 2 (column 4) for the available observers. The densities at this wavelength range from -0.09 to 1.01, with an average value of 0.38 ± 0.04. (We assume that the negative density values for HS2201 and HS2247 are due to noise, given that they are less than the standard error of each estimate.) These measured macular pigment densities can be compared with the best-fitting macular densities obtained by the fit of the full-spectrum model (see values in column 6 of Table 1 and below). Those values range from 0.01 to 0.83; and have an average value of 0.37 ± 0.03.

Fig. 6A shows the measured macular pigment densities plotted against the best-fitting densities obtained from the full spectrum model with best-fitting lens and macular pigment densities (see Section 3.5.1 below). The fitted regression line (thick continuous line) has a slope of 0.981 and a correlation coefficient, r^2, of 0.498. The thinner continuous lines show the 99% confidence intervals for the regression (i.e. the range within which the regression line would be expected to fall, for repeated measures, 99% of the time). Although the agreement between the measured and best-fitting densities is poor, the regression line is not significantly different from a line with a slope of 1 (i.e. perfect agreement, as shown by the diagonal dashed lines).

3.4. Lens pigment densities

To estimate lens densities, we measured rod spectral sensitivities at target wavelengths of 400, 420, 460 and 500 nm. We then determined the relative adjustment in lens density and the vertical shift that together mini-

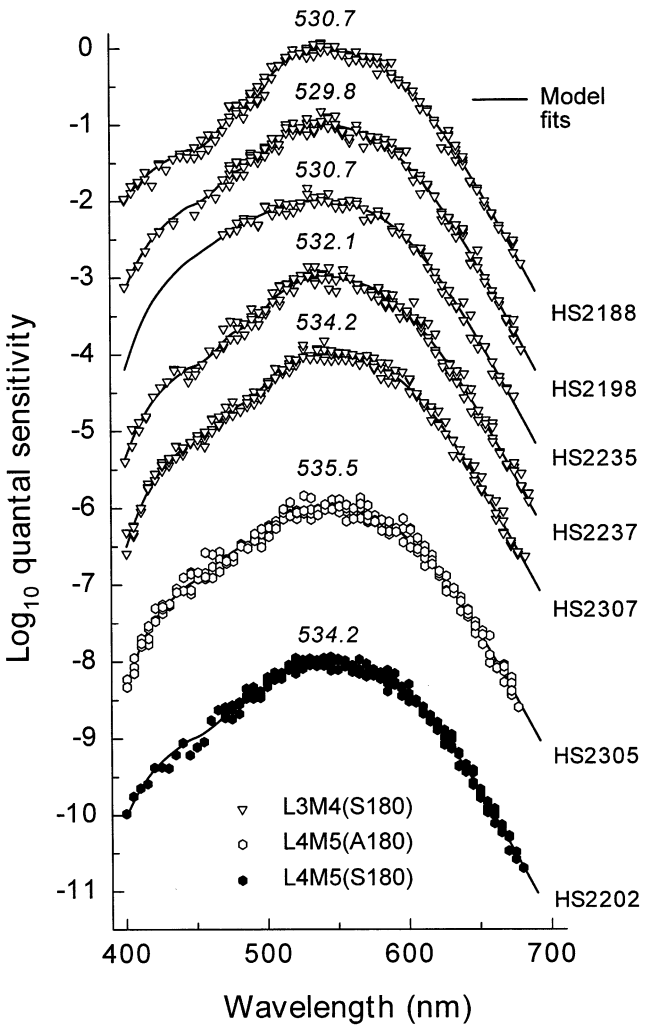

Fig. 2. Cone spectral sensitivity data for seven single-gene protanopes: four with an L3M4(S180) gene (▽); one with an L4M5(A180) gene (○); and one with an L4M5(S180) gene (filled hexagons). Other details as in Fig. 1.

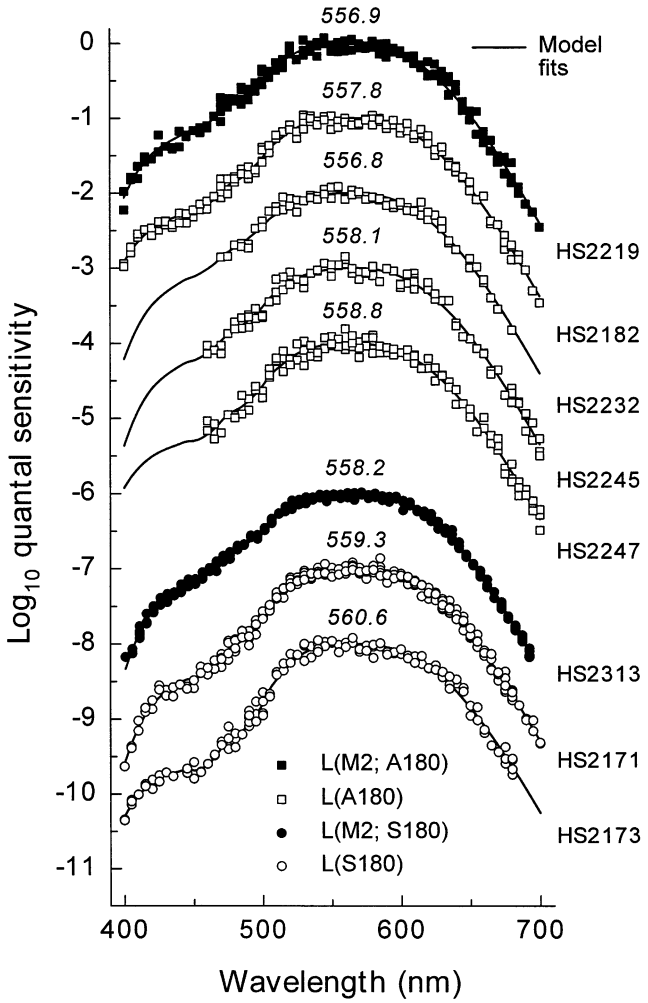

Fig. 3. Cone spectral sensitivity data for eight single-gene deuteranopes: one with an L(M2;A180) gene (■); four with an L(A180) gene (□); one with an L(M2;S180) gene (●); and two with an L(S180) (○). Other details as in Fig. 1.

mized the squared deviations between the subject's data and $V'(\lambda)$ (see Section 2). To reconstruct the absolute densities from the relative ones, we assumed that a zero relative adjustment was equivalent to a density at 400 nm of 1.48 (i.e. we assumed the mean density obtained from the best-fitting density analysis; see Table 1). The reconstructed values are tabulated in Table 2. They are tabulated, arbitrarily, as the density of the pigment at 400 nm.

Estimates of the lens pigment densities were obtained in all but eight of the dichromats (HS2241, HS2235, HS2245, HS2247, HS2220, HS2221, HS2243, HS2249). The lens pigment densities at 400 nm are listed in Table 2 (column 3) for the available observers. The values at this wavelength vary from 1.03 to 2.28; and have an average value of 1.56 ± 0.05. These measured lens pigment densities can be compared with the best fitting lens densities obtained by the fit of the full spectrum model (see values in column 5 of Table 1 and below). Those values range from 0.81 to 1.83, and have an average value of 1.48 ± 0.04. For the measured (Table 2) lens pigment densities there is a slight increase in density with age of the observer. This accords with the relative youth of the population sampled (28.1 ± 1.2; range from 16 to 45). The density of the crystalline lens at 400 nm increases linearly, but only gradually between 16 and 45 years of age (see Xu, Pokorny & Smith, 1997).

Fig. 6B shows the measured lens pigment densities plotted against the best-fitting densities obtained from the full spectrum model with best-fitting lens and macular pigment densities (see fit Section 3.5.1 below). The fitted regression has a slope of 0.717 and a r^2 of 0.375. The thinner continuous lines show the 99% confidence intervals for the regression. Once again, the agreement between the measured and best-fitting densities is poor, but the regression line is not significantly different from a line with a slope of 1.

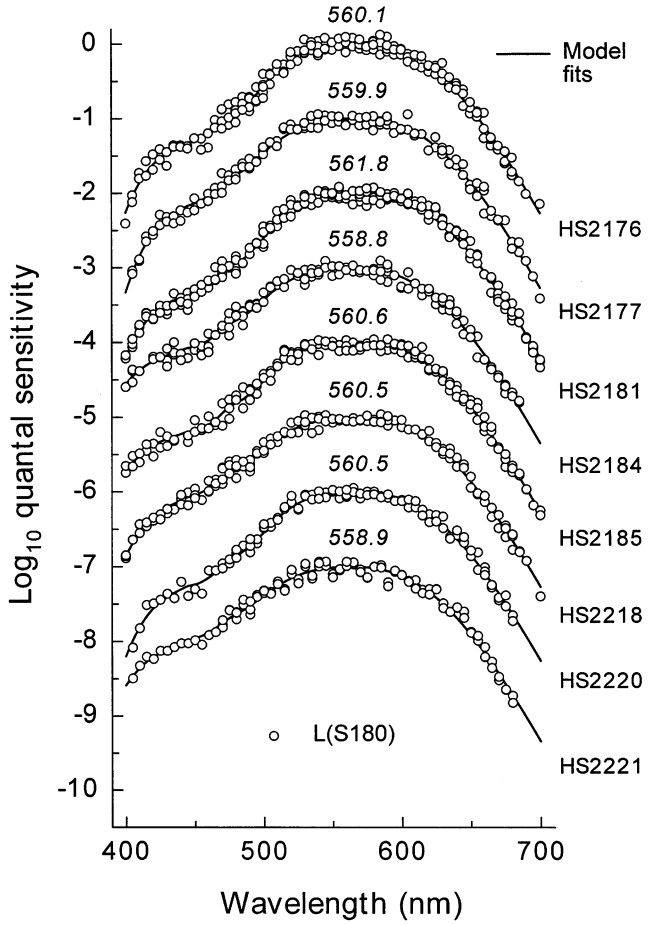

Fig. 4. Cone spectral sensitivity data for eight single-gene deuteranopes with an L(S180) (○). Other details as in Fig. 1.

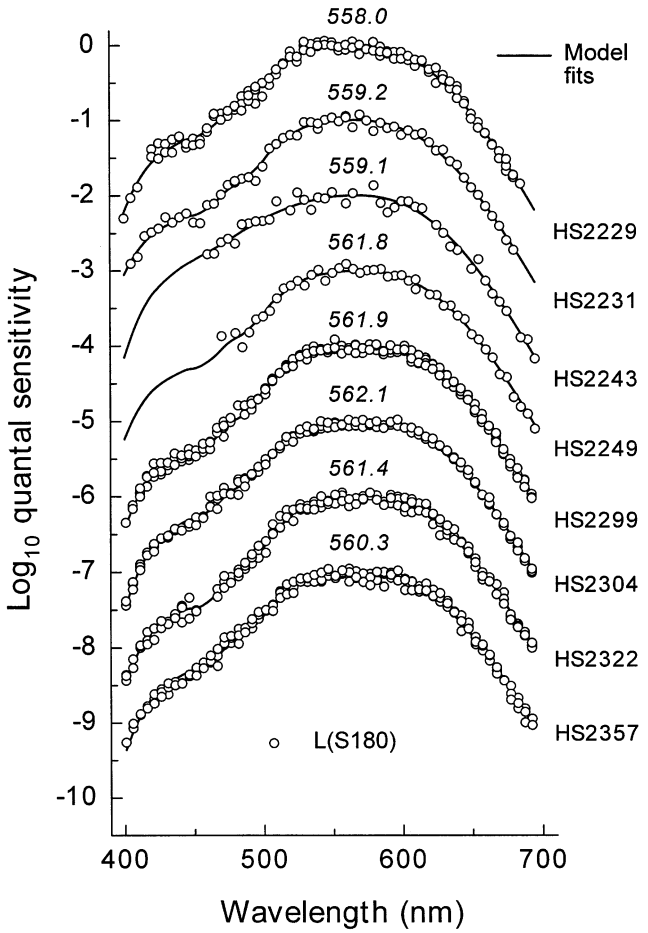

Fig. 5. Cone spectral sensitivity data for eight single gene protanopes with an L(S180) gene (○). Other details as in Fig. 1.

3.5. Peak absorbances (λ_{max} values)

As described in Section 2, the spectral sensitivity data for each observer were analyzed by three procedures to estimate the λ_{max} of the underlying longer wavelength cone photopigment.

3.5.1. Full-spectrum fit (with best-fitting lens and macular pigment densities)

In the first fitting procedure, we determined the best-fitting lens and macular pigment densities, as well as the spectral position of the underlying photopigment template from 400 to 700 nm. The fits of the model are shown as the continuous lines in Figs. 1–5, and the results are tabulated in Table 1. The λ_{max} values for protanopes range from 525.58 to 534.15 nm; whereas those for deuteranopes range from 556.81 to 562.09 nm.

3.5.2. Full-spectrum-fit (with measured lens and macular pigment densities)

In the second full-spectrum fit, measured lens and macular pigment densities were used.

The λ_{max} values and associated root mean square errors of the full-spectrum fit carried out with the measured lens and macular pigment densities are tabulated in Table 2. Fig. 7 compares the λ_{max} values so obtained with those obtained using best-fitting density values. The fitted regression line for protanopes (panel A) has a slope of 1.188 and an r^2 of 0.773; that for deuteranopes (panel B), a slope of 1.196 and an r^2 of 0.420. Although the agreement between the two analyses is poor, the results are not significantly different from perfect agreement (diagonal dashed lines).

The poor agreement seen in Fig. 7 could be caused either by the measured lens and macular pigment density values, which might be inaccurate, or by the best-fitting density values, which might be incorrect or skewed by the fitting procedure or model. We can determine which of these is flawed by estimating the λ_{max} values outside the spectral region in which individ-

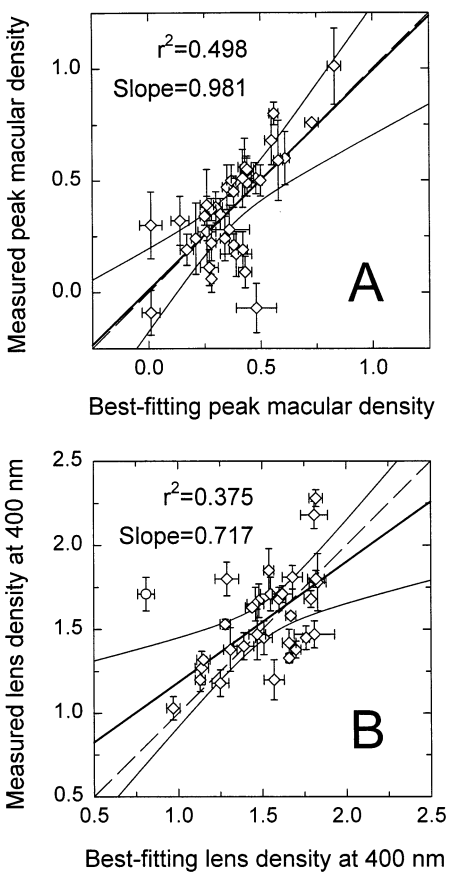

Fig. 6. Best-fitting densities from the full-spectrum analysis plotted against the measured densities for macular (A) and lens (B) pigments (◇). The regression line for the lens densities (A) has a slope of 0.981 and an r^2 of 0.498; whereas that for the macular pigment densities (B) has a slope of 0.717 and an r^2 of 0.375 (thicker continuous line). The thinner continuous lines show the 99% confidence intervals for the regressions lines. A perfect agreement between the two best-fitting and measured estimates is indicated by the dashed, diagonal lines. A single outlier (○) was excluded from the regression analysis for the lens density estimates.

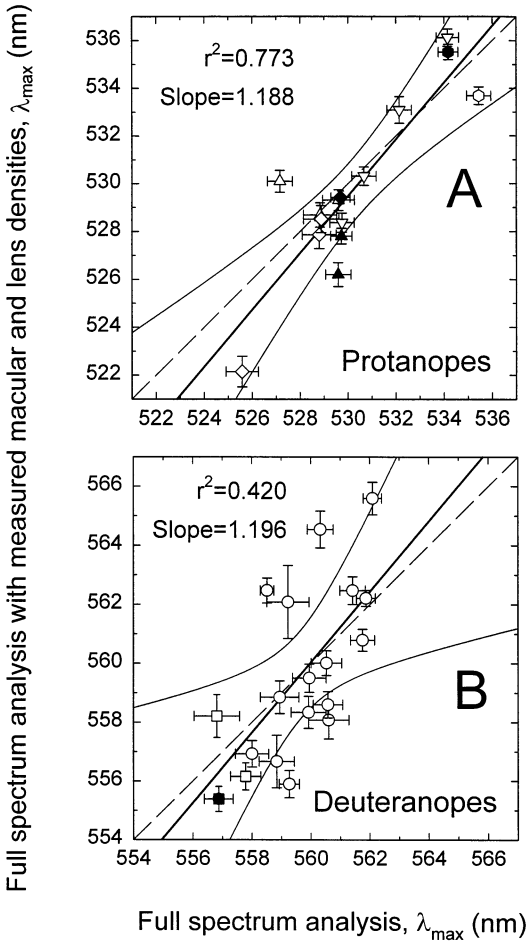

Fig. 7. λ_{max} values obtained from the full-spectrum analysis with estimated best-fitting lens and macular pigment densities plotted against those obtained from the full-spectrum analysis with individually measured lens and macular pigment densities. The regression line for protanopes (A) has a slope of 1.188 and an r^2 of 0.773, while that for deuteranopes (B) has a slope of 1.196 and an r^2 of 0.420 (thicker continuous lines). The 99% confidence intervals for the regressions are shown by the thinner continuous lines. Perfect agreement between the two estimates is indicated by the dashed, diagonal lines. Symbols as in Figs. 1–5.

ual differences in macular and lens pigment densities are important. This was done in the next fit.

3.5.3. Partial-spectrum-fit ($\geq$ 520 nm)

In the partial-spectrum fit, we fixed the macular and lens pigment densities at their mean best-fitting values, and determined only the spectral position of the underlying pigment template. The results are tabulated in Table 2.

The partial-spectrum fit acts as a control for the full-spectrum fits. Any distortions of the full-spectrum fits caused by inappropriate lens or macular pigment densities should result in clear discrepancies between the full-spectrum and partial-spectrum estimates of λ_{max}. These discrepancies will be in addition to the small differences that arise because mean rather than optimal lens and macular densities are assumed in the partial-spectrum fit (see Section 2).

Fig. 8 presents a comparison of the λ_{max} estimates obtained by the partial-spectrum fit and by the full-spectrum fit with best-fitting densities. The regression line (thick continuous line) for protanopes has a slope of 0.986 and an r^2 of 0.982; whereas that for deuteranopes has a slope of 0.844 and an r^2 of 0.942. The thin continuous lines indicate the 99% confidence intervals. For both protanopes and deuteranopes the correlations are high. The estimates for deuteranopes, however, fall along a regression line that is significantly shallower than a slope of one (dashed line). Thus, compared with a partial-spectrum fit, the full-spectrum fit tends to compress slightly the range of λ_{max} values of the deuteranopic observers.

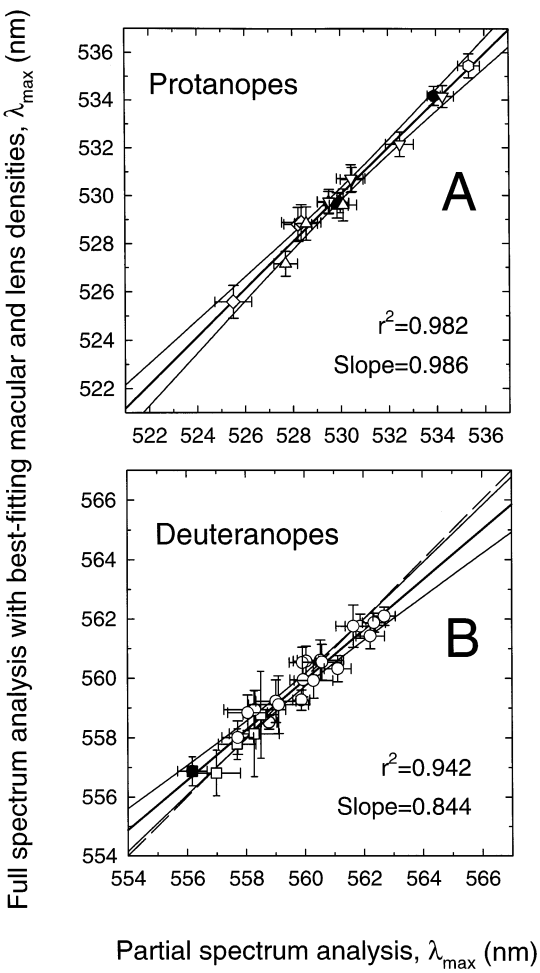

Fig. 8. λ_{max} values obtained from the partial-spectrum ($\geq$ 520 nm) analysis plotted against those obtained from the full-spectrum analysis. The regression line for protanopes (A) has a slope of 0.986 and an r^2 of 0.982, while that for deuteranopes (B) has a slope of 0.844 and an r^2 of 0.942 (thicker continuous lines). The thinner continuous lines show the 99% confidence intervals for the regressions. Perfect agreement is indicated by the dashed, diagonal lines. (Perfect agreement should not be expected since mean, rather than individual, lens and macular pigment density estimates are used in the partial-spectrum, but not full-spectrum, analysis.) Symbols as in Figs. 1–5.

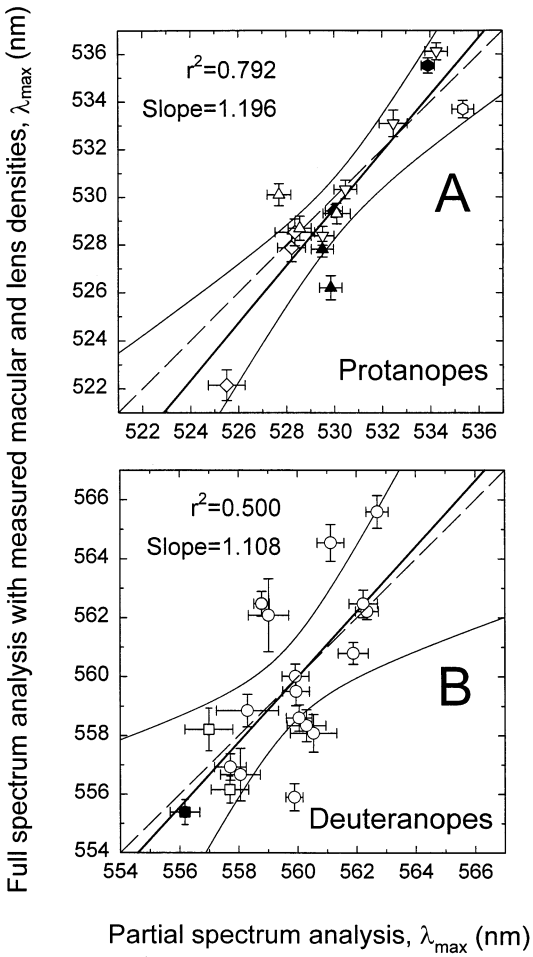

Fig. 9. λ_{max} values obtained from the partial-spectrum (≥ 520 nm) analysis plotted against those obtained from the full-spectrum analysis including incorporating individually measured densities. The regression line for protanopes (A) has a slope of 1.196 and an r^2 of 0.792, while that for deuteranopes (B) has a slope of 1.108 and an r^2 of 0.500 (thicker continuous lines). The thinner continuous lines show the 99% confidence intervals, and the dashed, diagonal lines indicate perfect agreement. Symbols as in Figs. 1–5.

Fig. 9 presents a comparison of the λ_{max} values obtained from the partial-spectrum (≥ 520 nm) fit and those obtained from the full-spectrum fit with measured densities. The regression line for protanopes has a slope of 1.196 and an r^2 of 0.792; whereas that for deuteranopes has a slope of 1.108 and an r^2 of 0.500 (thick continuous lines). Again, the thin continuous lines indicate the 99% confidence intervals. With measured macular and lens densities, the correlations, particularly for deuteranopes, are lower than those for the best-fitting densities. Nevertheless, the regression lines are not significantly different from a slope of one.

4. Discussion

By correlating the *X*-chromosome-linked visual pigment sequences and color vision phenotypes of a large population of red–green dichromats, we have characterized the spectral sensitivities in vivo of cones containing the normal human L- and M-cone pigments, as well as several different 5′L–3′M hybrid pigments. The correlation was simplified by the use of a population mainly consisting of single-gene male dichromats. Only three of the 40 dichromats in our investigations carried more than one opsin gene on their *X*-chromosome. However, the multiple opsin genes of these three observers did not differ significantly in the base sequences at the 19 critical codon positions examined. In one of the three, there were no differences between the opsin genes and in the other two, there were only differences at codon positions 111 and 116 in exon 2. Details of the genotype-phenotype correlations are fully provided elsewhere (Sharpe et al., 1998a), as is a discussion of how our in vivo results compare with results obtained using electroretinographic methods (Neitz, Neitz & Jacobs, 1995), with results obtained from recombinant human cone pigments produced in transfected cells and studied in detergent solution (Merbs & Nathans, 1992; Asenjo, Rim & Oprian, 1994), and with inferences based on a comparison of primate visual pigment gene sequences and cone spectral sensitivity curves (Ikeda & Urakubo, 1968; Neitz, Neitz & Jacobs, 1991; Williams, Hunt, Bowmaker & Mollon, 1992).

In the previous work, we estimated the peak absorbances (λ_{max}) of the underlying photopigment spectra from individual corneal spectral sensitivities by relying on best-fitting lens and macular pigment densities (see Table 1) to correct the data to the retinal level. In this work, we incorporated individually-measured lens and macular pigment densities. If the individual measures of density are themselves accurate, they should improve the accuracy of our λ_{max} estimates.

4.1. Spectral sensitivity analyses

We conducted two separate full-spectrum analyses of the complete spectral sensitivity data of each dichromatic observer to obtain the λ_{max} of the underlying longer wavelength cone photopigment. Both analyses depended upon correcting the spectral sensitivity data for the preretinal absorbing media of the lens and macular pigment, but they differed in whether the lens and macular pigment densities were best-fitting estimates obtained in the fitting procedure or individually-measured densities obtained independently. Given that the results provided by the two analyses differed, we undertook a third analysis, involving a partial-spectrum model that included only wavelengths ≥ 520 nm that are not significantly affected by inter-observer variability in lens and macular pigment filtering.

The partial-spectrum fit clearly supports the full-spectrum fit with best-fitting lens and macular pigment densities over the full-spectrum fit with measured densities. The individual lens and macular pigment density measurements, although they involved standard techniques, produced relatively inaccurate density estimates compared with those obtained from fitting density spectra to the flicker photometric spectral sensitivity data.

There are several reasons why the individually measured macular and lens pigment densities, could, in principle, be inaccurate. First, the dichromatic observers, who were relatively naïve and inexperienced, found the peripheral measurements much more challenging than the central ones. Second, the macular and lens density estimates were based on far fewer wavelengths than the spectral sensitivity measurements: the full spectral sensitivity measurements involved as many as 60 different wavelengths; whereas the macular pigment measurements involved only seven wavelengths and the lens measurements, only four. Third, the method of estimating macular pigment density ignores changes in photopigment optical density with eccentricity, the effect of which could slightly distort the macular density estimates and the λ_{max} fit (see Sharpe et al., 1998b).

It is not our intention to discourage the use of lens and macular pigment density determinations to correct corneal spectral sensitivities. It is important, however, that the density determinations be as accurate as the spectral sensitivity measurements. Thus, repeated measures at a comparable spectral density with well-trained subjects are required.

In order to obtain reliable and precise assays of the λ_{max} of the pigment variants, large population samples must be obtained. Inspection of the population data illustrates this point. For the pigment variant L(S180), comprising a large population of 18 observers, the size of the 95% confidence interval about the mean is 1.2 nm. Thus the average λ_{max} (560.3 nm) can be considered to accurately represent the true λ_{max} of the photopigment variant within about plus or minus 0.6 nm. In contrast, for the pigment variant L1M2(A180), comprising only three individuals, the size of the 95% confidence interval is 9.4 nm; or plus and minus about 4.7 nm, which is too large for making accurate predictions. The range of the estimate can be substantially improved, however, by including in the sample all those pigment variants whose absorbance maximum does not differ significantly from one another as determined psychophysically and by analysis of recombinant pigments: L1M2(A180), L1M2 $\pm$ M(A180), L2M3(A180), L2M3(A180) $\pm$ M(A180 (see Sharpe et al., 1998a). The group, now comprising nine individuals, has a 95% confidence interval of 2.6 nm. Thus, given the amount of noise in the data, accurate assays of the λ_{max} of pigment variants in vivo by our method requires repeated measures with highly-trained subjects.

In conclusion, in a previous study (Sharpe et al., 1998a), we estimated the λ_{max} values of several *X*-chromosome-linked normal and hybrid photopigments. We obtained them by correcting corneally measured spectral sensitivities back to the retinal level, after removing the effects of the macular and lens pigments and fitting a template of fixed shape to the dilute photopigment spectrum. In the previous study, we relied on best-fitting estimates of the lens and macular pigment densities. In this study, we compared those estimates of the λ_{max} with estimates based on individually measured lens and macular pigment densities. However, those comparisons and comparisons with a partial-spectrum fit (≥ 520 nm), which should not be significantly affected by lens and macular pigment filtering, indicate that the individually measured densities worsen rather than improve the fits. Presumably, the discrepancy arises because our techniques for measuring the lens and macular pigment densities rely on relatively few measurements made in peripheral retina; and, with naïve observers, these are less accurate than centrally measured flicker photometric sensitivities. We conclude that with this set of data the λ_{max} values derived with the best-fitting density estimates are overall the most reliable.

Acknowledgements

Supported by the Deutsche Forschungsgemeinschaft (Bonn) grants SFB 325 Tp A13, SFB 430 Tp A6 and Sh23/5-1 and a Hermann- und Lilly-Schilling-Stiftung-Professur (LTS), a National Institutes of Health grant EY 10206 (AS), and by the Howard Hughes Medical Institute (JN). We thank Clemens Fach, Gert Klausen and Andreas Reitner for assisting with the recruitment of the dichromats and with the spectral sensitivity measurements.

References

Alpern, M., & Wake, T. (1977). Cone pigments in human deutan color vision defects. *Journal of Physiology*, *266*, 595–612.

Asenjo, A. B., Rim, J., & Oprian, D. D. (1994). Molecular determinants of human red/green color discrimination. *Neuron*, *12*, 1131–1138.

De Vries, H. L. (1948). The fundamental response curves of normal and abnormal dichromatic and trichromatic eyes. *Physica*, *14*, 367–380.

Hecht, S. (1949). Brightness, visual acuity and color blindness. *Documenta Ophthalmologica*, *3*, 289–306.

Hsia, Y., & Graham, C. H. (1957). Spectral luminosity curves for protanopic, deuteranopic, and normal subjects. *Proceedings of the National Academy of Science USA*, *43*, 1011–1019.

Ikeda, M., & Urakubo, M. (1968). Flicker HRTF as test of color vision. *Journal of the Optical Society of America*, *58*, 27–31.

King-Smith, P. E., & Webb, J. R. (1974). The use of photopic saturation in determining the fundamental spectral sensitivity curves. *Vision Research*, *14*, 421–429.

Merbs, S. L., & Nathans, J. (1992). Absorption spectra of the hybrid pigments responsible for anomalous color vision. *Science*, *258*, 464–466.

Mitchell, D. E., & Rushton, W. A. H. (1971). Visual pigments in dichromats. *Vision Research*, *11*, 1033–1043.

Nathans, J., Merbs, S. L., Sung, C.-H., Weitz, C. J., & Wang, Y. (1992). Molecular genetics of human visual pigments. *Annual Review of Genetics*, *26*, 401–422.

Nathans, J., Thomas, D., & Hogness, S. G. (1986). Molecular genetics of human color vision: the genes encoding blue, green and red pigments. *Science*, *232*, 193–202.

Neitz, M., Neitz, J., & Jacobs, G. H. (1991). Spectral tuning of pigments underlying red–green color vision. *Science*, *252*, 971–974.

Neitz, M., Neitz, J., & Jacobs, G. H. (1995). Genetic basis of photopigment variations in human dichromats. *Vision Research*, *35*, 2095–2103.

Pitt, F. H. G. (1935). Characteristics of dichromatic vision. Medical Research Council Special Report Series, No. 200. London: His Majesty's Stationery Office.

Rayleigh, L. (1881). Experiments on colour. *Nature*, *25*, 64–66.

Ruddock, K. H. (1965). The effect of age upon colour vision II. Changes with age in light transmission of the ocular media. *Vision Research*, *5*, 47–58.

Rushton, W. A. H., Powell, D. S., & White, K. D. (1973). Exchange thresholds in dichromats. *Vision Research*, *13*, 1993–2002.

Sharpe, L. T., Stockman, A., Jägle, H., Knau, H., Klausen, G., Reitner, A., & Nathans, J. (1998a). Red, green, and red–green hybrid photopigments in the human retina: correlations between deduced protein sequences and psychophysically measured spectral sensitivities. *Journal of Neuroscience*, *18*, 10053–10069.

Sharpe, L. T., Stockman, A., Jägle, H., & Nathans, J. (1999). Opsin genes, cone photopigments, color vision and colorblindness. In K. Gegenfurtner, & L. T. Sharpe, *Color vision: from genes to perception*. Cambridge: Cambridge University.

Sharpe, L. T., Stockman, A., Knau, H., & Jägle, H. (1998b). Macular pigment densities derived from central and peripheral spectral sensitivity differences. *Vision Research*, *38*, 3233–3239.

Smith, V. C., & Pokorny, J. (1975). Spectral sensitivity of the foveal cone photopigments between 400 and 500 nm. *Vision Research*, *15*, 161–171.

Stiles, W. S. (1939). The directional sensitivity of the retina and the spectral sensitivity of the rods and cones. *Proceedings of the Royal Society of London*, *B127*, 64–105.

Stiles, W. S. (1953). Further studies of visual mechanisms by the two-colour threshold technique. *Coloquio sobre problemas opticos de la vision*, *1*, 65–103.

Stockman, A., MacLeod, D. I. A., & Johnson, N. E. (1993a). Spectral sensitivities of the human cones. *Journal of the Optical Society of America A*, *10*, 2491–2521.

Stockman, A., MacLeod, D. I. A., & Vivien, J. A. (1993b). Isolation of the middle- and long-wavelength sensitive cones in normal trichromats. *Journal of the Optical Society of America A*, *10*, 2471–2490.

Stockman, A., & Sharpe, L. T. (1999). Cone spectral sensitivities and color matching. In K. Gegenfurtner, & L. T. Sharpe, *Color vision: from genes to perception*. Cambridge: Cambridge University.

van Norren, D., & Vos, J. J. (1974). Spectral transmission of the human ocular media. *Vision Research*, *14*, 1237–1244.

Vos, J. J. (1972). Literature review of human macular absorption in the visible and its consequences for the cone receptor primaries. Netherlands Organization for applied scientific research, Institute for Perception, Soesterberg, The Netherlands.

Wald, G. (1964). The receptors of human color vision. *Science*, *145*, 1007–1016.

Williams, A. J., Hunt, D. M., Bowmaker, J. K., & Mollon, J. D. (1992). The polymorphic photopigments of the marmoset: spectral tuning and genetic basis. *EMBO Journal*, *11*, 2039–2045.

Willmer, E. N. (1950). Further observations on the properties of the central fovea in colour-blind and normal subjects. *Journal of Physiology*, *110*, 422–446.

Wyszecki, G., & Stiles, W. S. (1982). *Color science: concepts and methods, quantitative data and formulae* (2nd). New York: Wiley.

Xu, J., Pokorny, J., & Smith, V. C. (1997). Optical density of the human lens. *Journal of the Optical Society of America A*, *14*, 953–960.